TABLE III. Ratio of R to NR eigenvalues (in rydbergs) for several electron shells.

	$1s$	$4f$	$5d$	$6s$
$_{26}$Fe	1.008	...	...	...
$_{74}$W	1.09	0.81	0.84ᵃ	1.16
$_{78}$Pt	1.10	0.86	0.88	1.27
$_{80}$Hg	1.11	0.87	0.84	1.20
$_{92}$U	1.15	0.91	0.95	1.34

ᵃ Center of gravity not known, since only one j state is occupied.

for comparison. In Table II we list the R and NR eigenvalues for the incomplete 5d and 6s shells.

Taking the center of gravity of the two $5d$ levels, we find the difference of energy levels $6s-5d$ to be 0.39 eV in the R calculation and 2.80 eV in the NR calculation, yielding a net change in energy difference of 2.4 eV. The energy shifts are similar to those in uranium, though not as large.

Parenthetically it may be remarked that, for both elements, the R results are more reasonable than the NR, since we expect the eigenvalues of two competing incomplete shells to be close together, and this was true for the R results but definitely not for the NR results.

Cohen did R calculations not only for $_{92}$U and $_{78}$Pt, but also[5-7] for $_{80}$Hg, $_{74}$W, and $_{27}$Fe. NR calculations for these elements were available in the literature,[8-10] but since those for $_{80}$Hg and $_{74}$W were more than 25 years old, we carefully recomputed them. The accuracy achieved by Hartree and Hartree in their results for $_{80}$Hg was remarkable, considering that only desk calculators were available to them in 1935. In Table III we list the R/NR ratios for the $1s$, $4f$, $5d$, and $6s$ electrons, to show how the relativistic effects vary with Z.

Apparently the indirect relativistic effect on electrons of high angular momentum is stronger when those electrons are near the surface. It would be worthwhile to do NR and R calculations for $_{64}$Gd in the ground-state configuration $4f^{7}5d6s^{2}$ to determine whether or not the shifts in the $4f$ and $5d$ energy levels are significant for the rare earths.

[5] S. Cohen, Rand Corporation Research Memorandum, RM-2272—AEC, 1958 (unpublished).
[6] S. Cohen, Phys. Rev. 118, 489 (1960).
[7] S. Cohen, Rand Corporation Research Memorandum, RM-2406—AEC, 1959 (unpublished).
[8] D. R. Hartree and W. Hartree, Proc. Roy. Soc. (London) A149, 210 (1935).
[9] M. F. Manning and J. Millman, Phys. Rev. 49, 848 (1936).
[10] F. Stern, Phys. Rev. 104, 684 (1956).

Polarization of Optical Radiation Induced by Electron Impact on Helium*

R. H. Hughes, R. B. Kay,† and L. D. Weaver
Physics Department, University of Arkansas, Fayetteville, Arkansas
(Received 28 September 1962)

An investigation of the polarization of the atomic line radiation induced by electron impact on helium has been undertaken. Experimental data have been obtained on the polarization of several lines as a function of both electron energy and pressure. Secondary excitation processes, such as collision of the second kind and radiative transfer (cascade), are found to play an important role in the polarization. Expressions are derived for the analysis of the pressure effects on the polarization. Gas-kinetic collision cross sections involving atoms in excited states have been determined by observing the depolarization as the gas pressure increases.

INTRODUCTION

IF an excitation mechanism, such as electron impact or absorption of polarized resonance radiation, can simultaneously excite and orient an atom with respect to a given direction, then the radiation emitted when the atom de-excites can exhibit polarization.

In particular, consider the polarization of the light excited by a well-collimated beam of monoenergetic electrons. The quantity termed the polarization, P, is defined through the equation

$$P = (I_{11} - I_{\perp})/(I_{11} + I_{\perp}),$$

* Supported by the Air Force Office of Scientific Research.
† Now at the McDonnell Aircraft Corporation, St. Louis, Missouri.

where I_{11} and $I_{\perp}$, in an observation direction perpendicular to the beam, are intensities of the radiation with the electric vectors, respectively, parallel and perpendicular to the beam direction.

The phenomenon of the polarization of atomic radiation induced by electron impact can most easily be understood qualitatively by considering Lamb's example[1] of a spinless hydrogen atom in the $1s$ ground state being struck by a spinless electron. If the bombarding electron energy is the threshold energy for exciting the $2p$ state and the electron succeeds in exciting the $2p$ state, then this electron (or exchanged electron) comes to rest. The linear momentum imparted to the

[1] W. E. Lamb, Phys. Rev. 105, 559 (1957).

atom will be in the direction of the incident electron, but the atomic angular momentum imparted will be in the direction perpendicular to the incident electron direction. This corresponds to exciting the magnetic quantum state, $m_1 = 0$ with respect to the incident-electron direction. When the atom de-excites to the ground state, the change in the magnetic quantum number is zero, which corresponds to the π transition in the Zeeman effect. This would indicate a 100% polarization in the direction parallel to the incident-beam direction when viewed perpendicularly to the beam direction. As the incident-electron energy increases, the scattered electron carries off angular momentum, thus populating the $m_1 = \pm 1$ states as well, which results in the appearance of the "Zeeman" σ components. This is reflected as a decrease in the percentage polarization of the emitted radiation. As the bombarding energy is increased, the polarization will pass through the value zero and become negative when the fast electrons begin to preferentially populate the $m_1 = \pm 1$ states.

Percival and Seaton[2] have derived expressions for the polarization induced by electron impact under the assumptions: (1) LS coupling is valid; (2) the excitation potential does not involve spin coordinates; and (3) the ground state has zero orbital angular momentum. Calculation of the polarization requires knowledge of the probability of populating states with particular M_L values. In general, the results indicate that the absolute value of the polarization should reach a maximum at threshold, but instead one generally finds a maximum is reached a few volts above threshold, with the polarization decreasing as threshold is approached. This behavior was first noted for Hg.[3,4] No satisfactory explanation has been forthcoming regarding this anomalous low-energy result.

Experimental work has been reported on the polarization of radiation produced by electron impact on helium by several authors.[5-8]

DERIVATION OF SOME GENERAL EXPRESSIONS FOR POLARIZATION ANALYSIS

Percival and Seaton develop expressions for the polarization of radiation induced by electron impact on helium-like atoms but do not consider secondary excitation processes such as collision of the second kind and cascade. The effect of disorienting gas-kinetic

[2] I. C. Percival and M. J. Seaton, Phil. Trans. Roy. Soc. (London) 251, 113 (1958).

[3] H. W. B. Skinner, Proc. Roy. Soc. (London) A112, 642 (1926).

[4] H. W. B. Skinner and E. T. S. Appleyard, Proc. Roy. Soc. (London) A117, 224 (1927).

[5] G. G. Dolgov, Opt. Spectr. (U.S.S.R.) 6, 469 (1959).

[6] R. H. Hughes, R. B. Kay, and L. D. Weaver, Fourteenth Annual Gaseous Electronics Conference, Schenectady, New York, 1961 (unpublished).

[7] C. B. Lucas, Ph.D. thesis, University College, London, 1961 (unpublished).

[8] R. H. McFarland and E. A. Soltysik, Phys. Rev. 127, 2090 (1962).

collisions needs to be taken into account when studying the polarization as a function of the pressure. Some discussion of the depolarization of radiation induced by gas-kinetic collisions can be found in Mitchell and Zemansky.[9]

The following derivation uses a notation similar to that of Percival and Seaton.

Let β represent a particular quantum state of an excited level b of an atom being subjected to electron bombardment. In the LS coupling scheme using $SLJM_J$ as the appropriate angular momenta, the level b is characterized by a particular set of the quantum numbers ΔSLJ where Δ denotes quantum numbers other than those associated with angular momenta. The state β is then characterized by a particular M_J in the level. The state β' is defined as a state belonging to b but having an M_J value different from β. For clarity only, it is assumed for the time being that the other multiplet levels belonging to the same ΔSL can be resolved spectroscopically.

Considering the different rates of populating and depopulating the state β, one finds the following:

$$dN(\beta)/dt = (i/e)nlQ(\beta), \qquad (1)$$

which represents the rate of populating the state by electron impact where $N(\beta)$ is the number of atoms in state β, i/e is the number of electrons/sec, n is the ground-state atom density, l is the length of electron beam under observation, and $Q(\beta)$ is the electron excitation cross section.

$$dN(\beta)/dt = (i/e)nlf_b(n)/(2J_b+1), \qquad (2)$$

which represents the rate of populating the state by some secondary process which will be independent of M_J and will be a function of n alone. Such a process might be collisions of the second kind (excitation transfer such as in the reaction, $n\,^1P \rightarrow n\,^1D$). This does not include absorption of resonance radiation which is complicated by orientation effects in the absorption process.

$$dN(\beta)/dt = \bar{v}n\sigma_b N(\beta')/(2J_b+1), \qquad (3)$$

which represents the rate of populating the state by thermal gas-kinetic collisions in which atoms in excited states $\beta' \neq \beta$ are placed into state β. Here $\bar{v}$ is the mean thermal velocity, σ_b is the disorienting collision cross section between the excited atom and a ground-state atom, and $N(\beta')$ is the number of atoms in all states $\beta' \neq \beta$. Since there are $2J_b+1$ states in the level b, then the probability of changing a β' into β is $1/(2J_b+1)$.

$$dN(\beta)/dt = \sum_\alpha A(\alpha\beta)N(\alpha), \qquad (4)$$

which represents the rate of populating the state by radiative transfer (cascade) from a higher state α

[9] A. C. G. Mitchell and M. W. Zemansky, Resonance Radiation and Excited Atoms (Cambridge University Press, New York, 1934), p. 308.

belonging to level a. $A(\alpha\beta)$ is the radiative transition probability connection α to β.

$$dN(\beta)/dt = -N(\beta)/T_b, \tag{5}$$

which represents the rate of depopulating the state by radiative processes. T_b is the mean lifetime of the state.

$$dN(\beta)/dt = -\bar{v}n\sigma_b N(\beta)[1-1/(2J_b+1)], \tag{6}$$

which represents the rate of depopulating the state by thermal collisions. The probability of removal from a particular state is $1-1/(2J_b+1)$.

If the cascade (Process 4) is neglected and equilibrium is assumed, then

$$\frac{i}{e}nl\left[Q(\beta)+\frac{f_b(n)}{2J_b+1}\right]+\frac{\bar{v}n\sigma_b N(\beta')}{2J_b+1}$$

$$=\frac{N(\beta)}{T_b}+\bar{v}n\sigma_b N(\beta)\left[1-\frac{1}{2J_b+1}\right]. \tag{7}$$

Transposing and using $N(\beta')+N(\beta)=N(b)$, where $N(b)$ is the total number of atoms in the level, the result is

$$\frac{i}{e}nl\left[Q(\beta)+\frac{f_b(n)}{2J_b+1}\right]+\frac{\bar{v}n\sigma_b N(b)}{2J_b+1}=N(\beta)\left[\frac{1}{T_b}+\bar{v}\sigma_b n\right]. \tag{8}$$

(It is somewhat interesting to note from this last expression that the rate of populating the state β by gas kinetic collisions is equal to the rate of depopulating the state by this same process when $N(b)=(2J_b+1)$ $\times N(\beta)$. This condition will be fulfilled for "natural excitation"; that is, when the number of atoms in the different states of the same level are equal. This, of course, is an expected result.)

Observing in a direction perpendicular to the monoenergetic electron beam the atomic line radiation which is produced when β decays, let $I_{||}=D\sum_\beta A_z(\beta)N(\beta)$ and $I_\perp=D\sum_\beta A_y(\beta)N(\beta)$. $I_{||}$ and $I_\perp$ are the intensities of the spectral line under study with the electric vector, respectively, parallel and perpendicular to the electron beam direction; D is a constant; and $A_z(\beta)$ and $A_y(\beta)$ are components of the transition probability connecting the state β with the lower state involved in the transition and are characterized by the polarization direction.

Using $\sum_\beta A_z(\beta)=\sum_\beta A_y(\beta)=(2J_b+1)A(b)/3$ where $A(b)$ is the total transition probability and $N(b)A(b)=(I_{||}+2I_\perp)/D=(I_{||}+I_\perp)(3-P)/2D$, it follows that

$$I_{||}+I_\perp=$$

$$\frac{(i/e)nlDT_b\{\sum_\beta Q(\beta)[A_z(\beta)+A_y(\beta)]+\frac{2}{3}f_b(n)A(b)\}}{1+\bar{v}\sigma_b nPT_b/3}. \tag{9}$$

Letting $I_{||}+I_\perp=(i/e)nlDT_bA(b)\frac{2}{3}Q'(b)$ where $Q'(b)$ is

the apparent cross section for populating b as measured perpendicular to the beam, the polarization becomes

$$P=P_0/[Q'(b)/Q_0'](1+\bar{v}\sigma_b nT_b), \tag{10}$$

where Q_0' is the apparent cross section for populating b at very small pressures. [Equation (10) can be obtained more simply, of course, without reference to Eq. (9). We include Eq. (9) only to show the behavior of the generally experimental quantity, $I_{||}+I_\perp$, with polarization.]

The addition of the cascade process into β from a state α, for which cascade into α can be neglected, makes Eq. (8) become

$$\frac{i}{e}nl\left[Q(\beta)+\frac{f_b(n)}{2J_b+1}\right]+\frac{\bar{v}n\sigma_b N(b)}{2J_b+1}$$

$$+\left\{\sum_\alpha A(\alpha\beta)\frac{i}{e}nl\left[Q(\alpha)+\frac{f_a(n)}{2J_a+1}\right]+\frac{\bar{v}\sigma_a nN(a)}{2J_a+1}\right\}$$

$$\times\left(\frac{1}{T_a}+\bar{v}\sigma_a n\right)^{-1}=N(\beta)\left[\frac{1}{T_b}+\bar{v}\sigma_b n\right]. \tag{11}$$

We find then

$$I_{||}-I_\perp=in\left[(B_{||}-B_\perp)+\frac{(C_{||}-C_\perp)}{1+\bar{v}\sigma_a nT_a}\right]$$

$$\times(1+v\sigma_b nT_b)^{-1}, \tag{12}$$

where the B's and C's are associated with the direct excitation of b and the cascade from direct excitation of a, respectively.

In the special case where $C_{||}\approx C_\perp$ and $n\approx 0$, the polarization becomes

$$P\approx P_b/1+Q(a)T_aA(ab)/Q(b), \tag{13}$$

where P_b is the polarization expected without cascade. $Q(b)$ is the value for the cross section for direct excitation into b, but if one measures instead an apparent cross section $Q'(b)=Q(b)+A(ab)T_aQ(a)$, Eq. (12) becomes

$$P\approx P_b[1-A(ab)T_aQ(a)/Q'(b)]. \tag{14}$$

Taking into account several cascading levels, the polarization is

$$P\approx P_b\left(1-\frac{\sum_k A(a_kb)T_{a_k}Q(a_k)}{Q'(b)}\right). \tag{15}$$

EXPERIMENTAL APPARATUS

An electron gun from a Sylvania 3BP1 cathode-ray tube was employed. The deflection plates were removed and the final anode was positioned beneath a set of beam entrance holes (Fig. 1) which led to the collision chamber. The beam could be focused so that a parallel beam entered the observation chamber without striking

metal surfaces which would produce secondary electrons in the observation region.

The thermal energy spread in the beam can be easily calculated using the Maxwell-Boltzman energy distribution function. This shows that 90% of the electrons in the space charge around the cathode are in the range from 0 to 0.3 eV.

The excitation of the gas was to take place in field-free surroundings since either magnetic or electrostatic fields would affect the atom orientation during the lifetime of the excited state. The existence of fields would also affect the beam energy and direction. This led to the chamber system proper being made from low-carbon steel with the interior surface coated with colloidal graphite. It was hoped that electric and magnetic shielding would be maintained in the chamber system.

Figure 1 shows the electron beam apparatus, including the collision chamber. The system was differentially pumped so that pressures of the order of 0.1μ of Hg could be maintained in the lower section which contained the electron gun while the pressure in the excitation chamber was of the order of 10μ. Incidentally, having the small beam entrance apertures not only reduced the gas flow but also reduced the amount of ultraviolet resonance radiation produced in the lower section entering the observation region.

Helium was let into the collision chamber *via* a variable leak valve and liquid-air-cooled charcoal trap. Pressure gauges were mounted on top of this chamber: a Pirani gauge, an ionization gauge, and later a McLeod gauge. A fused-quartz window was mounted on the front of the chamber for collision radiation observation and a glass window was mounted on the side of the chamber for visual beam alignment. On the top and centered on the beam axis was mounted a deep Faraday
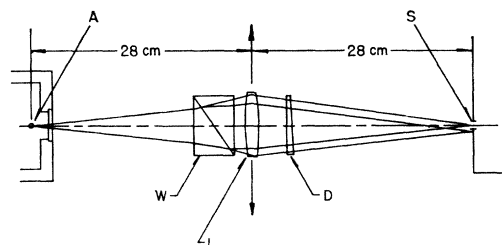
FIG. 2. Optical system. (A) collision region, (W) Wollaston prism, (L) 14-cm-focal length lens, (D) depolarizing wedge, (S) spectrometer entrance slit.

cup which caught the beam, and was used to measure the beam current.

A 14-cm focal length fused-quartz lens was placed 28 cm in front of the source and an image of the electron beam was focused on the entrance slit of a Jarrell-Ash model 82–000 scanning spectrometer located at a distance of 28 cm from the lens. A EMI 6256B photomultiplier was used at the spectrometer exit slit.

As the impact radiation consists of components polarized parallel and perpendicular to the beam axis, a Wollaston prism was used to separate these components. In order to separately compare these two images they were scanned across the entrance slit of the spectrometer. This scanning was accomplished by mounting the lens on a motor driven pendulum.

Since the spectrometer treats the two modes of polarization differently upon reflection (i.e., their reflection coefficients are not the same), special provisions were made to depolarize the light before it encountered any reflecting surface. This was accomplished by a special quartz wedge.[10] Figure 2 graphically illustrates the optical system.

To check the beam energy, a variable negative supply was placed in the beam current measuring circuit so that a retarding potential could be placed on the Faraday cup. The cutoff voltage was then used to determine the mean energy of the electrons in the collision chamber. This value could be determined to within approximately $\pm\frac{1}{4}$ V in the 24–28-V region. Figure 3 shows a retarding potential vs beam current plot for an accelerating voltage of 47.5 V. Although Fig. 3 seems to indicate an energy spread on the order

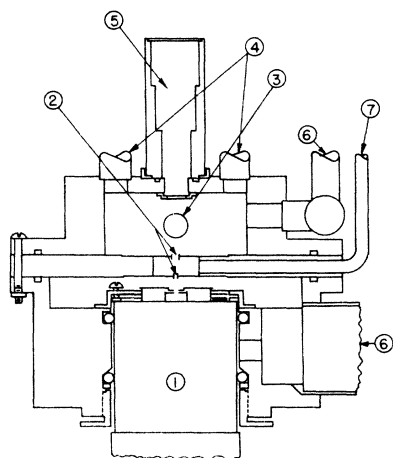FIG. 3. Beam current (I) vs retarding potential (E) (accelerating potential 47.5 V).

FIG. 1. Collision chamber system. (1) electron gun, (2) beam entrance holes, (3) observation window, (4) vacuum gauge supports, (5) Faraday cup, (6) pump outlets, and (7) differential pumping outlet.
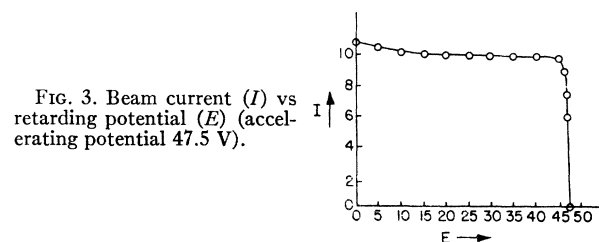
[10] R. H. Hughes, Rev. Sci. Instr. **31**, 1156 (1960). Note: A similar depolarizer has been described by W. Hanle, Z. Instrumentenk, **51**, 488 (1931). We appreciate Dr. Hanle's private communication pointing out our oversight.
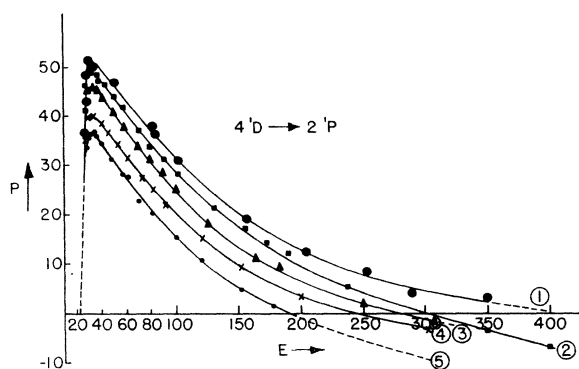
FIG. 4. Polarization (P) in $\%$ vs electron energy (E) in eV for the $4\,^1D \to 2\,^1P$ transition ($\lambda 4922$ Å) at pressures of (1) 0.5μ, (2) 5μ, (3) 10μ, (4) 20μ, and (5) 30μ.

of a volt or so, it may be that the actual spread is considerably less. Much of the apparent spread may likely be a product of space-charge effects at the Faraday cup when the retarding potential is close to cutoff.

POLARIZATION RESULTS AND INTERPRETATION

A. $\lambda 4922$ $(4\,^1D \to 2\,^1P)$ and $\lambda 4388$ $(5\,^1D \to 2\,^1P)$

The polarization for these lines at threshold theoretically should be $+60\%$.

Figures 4 and 5 show plots of polarization vs energy for $4\,^1D \to 2\,^1P$ and $5\,^1D \to 2\,^1P$ transitions at various pressures. The low-energy part of the curve shows a characteristic maximum and a monotonic falloff as threshold is approached. One of the interesting features is the fact that the value of the crossover point (where the polarization goes through zero at higher energies) seems to be pressure dependent, the crossover moving to higher energies as the pressure is decreased.

The value of the crossover would not be expected to be pressure dependent if the excitation is due only to the primary process of electron impact. In such a case crossover chould occur at a particular energy with only the slope of the curve through the cross over changing with pressure.
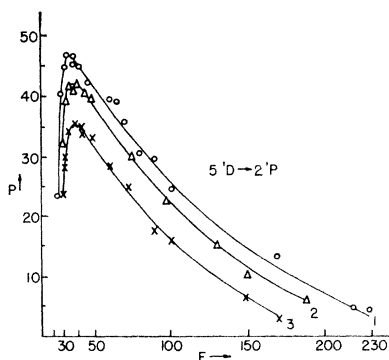

FIG. 5. Polarization (P) in $\%$ vs electron energy (E) in eV for the $5\,^1D \to 2\,^1P$ transition ($\lambda 4387$ Å) at pressures of (1) 3.5μ, (2) 10μ, (3) 20μ.
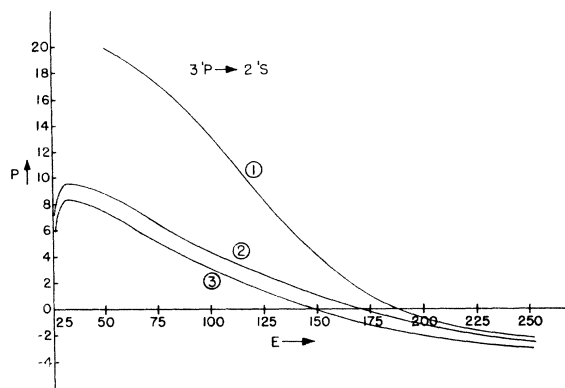

FIG. 6. Polarization (P) in $\%$ vs electron energy (E) in eV for the $3\,^1P \to 2\,^1S$ transition ($\lambda 5015$ Å) at pressures of (1) 5μ, (2) 10μ, and (3) 20μ.

It seems reasonable that cascade from $^1F_3$ levels may offer a possible explanation. The cascade from these levels to the $^1D_2$ level could contribute appreciably to the polarization of the $^1D \to {}^1P$ transition. For example, considering only the cascade population of a $^1D_2$ level from a $^1F_3$ level in which only the $m_J = 0$ state is excited by direct electron impact, a polarization equal to $+50\%$ can be calculated for the $^1D_2 \to {}^1P_1$ transition. (The expected polarization of the $^1F \to {}^1D$ transition would also be $+50\%$.)

The cascade effect from F levels to low-lying D levels represents almost the only mode of radiative decay open to F levels. The size of the effect depends of course on the relative cross sections for direct excitation of the F levels and D levels which, however, appear small.[11]

Nevertheless, consider the possible effect of ^1F cascade on the crossover point for a $^1D \to {}^1P$ transition. The crossover occurs when $I_{11} - I_\perp = 0$ or when Eq. (13) is set equal to zero. In this case the B's and C's of Eq. (12) are associated with a $n\,^1D$ and a cascading ^1F, respectively. If cascading were negligible, then the crossover implies $B_{11} - B_\perp = 0$ which will occur at some energy E_1. On the other hand, $C_{11} - C_\perp = 0$ will occur at some other energy E_2. The ^1F state represents a state of higher angular momentum, and it seems reasonable that the population of the high-valued magnetic substates of this level will begin at relatively higher electron energies where the electron can carry away more angular momentum. If this is so, then $E_2 > E_1$. Further, the effect of disorienting atom-atom collisions will be fairly great on the cascading ^1F level since the lifetime of ^1F level is long and also the atom-atom collision cross section is expected to be large for the high lying ^1F. Thus, as the pressure is increased, the crossover moves toward E_1 while a decrease in pressure moves the crossover away from E_1 as the cascading ^1F states contribute relatively more to the quantity $I_{11} - I_\perp$. Figure 4

[11] H. S. W. Massey and E. H. S. Burhop, *Electronic and Ionic Impact Phenomena* (Oxford University Press, New York, 1952).

indicates then that the crossover point for the $4\,^1D \to 2\,^1P$ transition would occur at $E < 200$ eV without cascade.

B. λ5015 Å $(3\,^1P \to 2\,^1S)$

The theoretical polarization at threshold for this line is $+100\%$. Figure 6 shows the experimental results for this line.

Analyzing the polarization for this line is extremely difficult. The $3\,^1P$ state is optically connected to the ground state and imprisonment of resonance radiation becomes a factor. We plotted the polarization vs pressure for both the $3\,^1P \to 2\,^1S$ and $4\,^1P \to 2\,^1S$ transitions at 35 V and found the plot to be linear up to about 10μ. We found that $(I_{11}-I_{\perp})/in$ increases with pressure presumably because of the scattering of polarized resonance radiation. The apparent cross section for this line increases rapidly with pressure accounting for the large reduction in the magnitude of the polarization as the pressure is increased.

The behavior of the position of the crossover point as a function of the pressure is interesting although not as pronounced as with other lines. The motion of the crossover point to greater energies as the pressure is decreased is to be expected if cascade from higher ^1D levels is noticeable, since we have previously seen that the polarization of the $n\,^1D \to 2\,^1P$ behaves in this same fashion. Such a cascading effect would be expected to be small but perhaps noticeable around the crossover point. Using the 108-V data of Gabriel and Heddle,[12] the contribution to the total population of the $3\,^1P$ level by cascade from higher ^1D levels is only about 2% of that from direct excitation. However, around the crossover point the effect of cascade on $I_{11}-I_{\perp}$ may be observable. In other words, although $B_{11} \gg C_{11}$ and $B_{\perp} \ll C_{\perp}$ [Eq. (12)], it may be when $B_{11} \approx B_{\perp}$ that $C_{11}-C_{\perp}$ becomes more comparable to $B_{11}-B_{\perp}$. This becomes reasonable by comparing the polarization curves for $4\,^1D \to 2\,^1P$ (Fig. 4) with the $3\,^1P \to 2\,^1S$ curves (Fig.
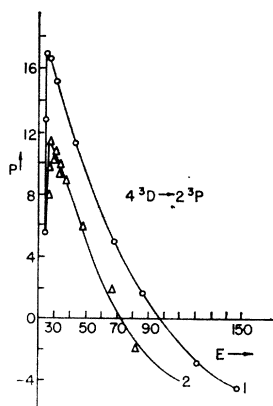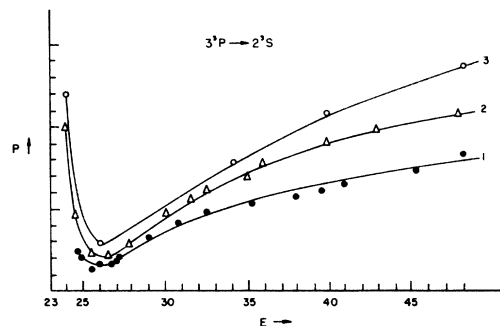

FIG. 8. Polarization (P) in $\%$ vs electron energy (E) in eV for the $3\,^3P \to 2\,^3S$ transition (λ3889 Å) at pressures of (1) 30μ, (2) 10μ, and (3) 0.5μ.

6). The crossover points in Fig. 4 occur at a much higher energies than for the $3\,^1P \to 2\,^1S$ line. At the crossover energy for the $3\,^1P \to 2\,^1S$, the $4\,^1D \to 2\,^1P$ transition exhibits appreciable polarization for corresponding pressure.

C. λ4471 Å $(4\,^3D \to 2\,^3P)$

At threshold, this line should theoretically exhibit a polarization of 31.7%. Figure 7 shows again the characteristic monotonic falloff of the polarization after the maximum is reached a few volts above threshold.

The crossover point is again pressure dependent. Our interpretation of the pressure dependence of the crossover is again based on cascade. In this case, high-lying ^3P level and ^3F levels cascade to the $4\,^3D$ level and contribute more heavily to $I_{11}-I_{\perp}$ at lower pressures than at higher pressures where disorienting collisions appreciably affect these higer states.

We can place an upper limit on the crossover of this line in the absence of cascade effect at 70 V. (It is

FIG. 7. Polarization (P) in $\%$ vs electron energy (E) in ev for the $4\,^3D \to 2\,^3P$ transition (λ4471 Å) at pressures of (1) 5μ, and (2) 10μ.

[12] A. H. Gabriel and D. W. O. Heddle, Proc. Roy. Soc. (London) A258, 124 (1960).
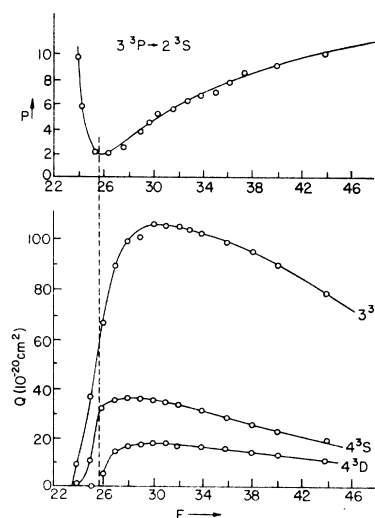

FIG. 9. The upper curve is polarization (P) in $\%$ vs energy (E) for the λ3889 Å line at 10μ while the lower curves are plots of apparent level excitation for the $3\,^3P$, $4\,^3S$, and $4\,^3D$ levels at 10μ.
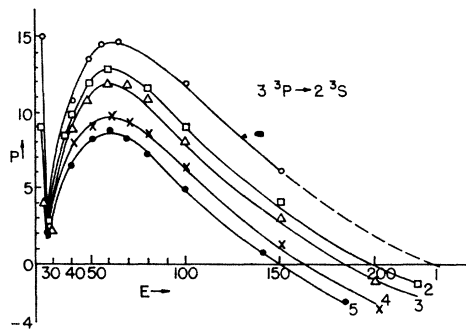
FIG. 10. Polarization (P) in $\%$ vs vs electron energy (E) in eV for the $\lambda 3889$ Å line for pressures of (1) 0.4μ, (2) 5μ, (3) 10μ, (4) 20μ, and (5) 30μ.

quite likely much less than this since this represents the crossover at only 10μ pressure.)

D. λ3889 Å $(3\ {}^3P \rightarrow 2\ {}^3S)$

This line should theoretically show a polarization of 36.6% at threshold. Figure 8 shows the very interesting behavior of this line at low energy. The low-energy minimum in the polarization was first noted by Lamb and Maiman.[13] Dolgov, however, published an entirely different looking polarization curve that did not show this behavior. Our work (and that of McFarland[8]) confirms the minimum. It occurs in our apparatus at about 26 V.

This $3\ {}^3P$ level is quite heavily populated by cascade, particularly from ${}^3S$ levels. Cascade from directly excited ${}^3S$ levels should tend to lower the polarization of $3\ {}^3P \rightarrow 2\ {}^3S$ since there should be no preference shown in populating the states of the ${}^3S$ levels by electron impact. Furthermore, the maximum in the excitation curve of ${}^3S$ levels appears at an energy close to the minimum in the polarization curve for $3\ {}^3P \rightarrow 2\ {}^3S$. Excitation curves (Fig. 9) were obtained for $4\ {}^3S \rightarrow 2\ {}^3P$, $4\ {}^3D \rightarrow 2\ {}^3P$ and $3\ {}^3P \rightarrow 2\ {}^3S$. The maxima of these excitation curves were normalized using the apparent cross-section values found by Stewart and Gabathuler.[14] The polarization expected if cascade were not present (P_b) was calculated for 26 eV using Eq. (15). Since the polarization shown by $4\ {}^3D \rightarrow 2\ {}^3P$ is small in this energy region, cascade of ${}^3D$ as well as ${}^3S$ was taken into account under the assumption that cascade from these levels contributes nothing to $I_{11} - I_1$ for $3\ {}^3P \rightarrow 2\ {}^3S$. Transition probabilities from the tables of Gabriel and Heddle[12] were used while apparent cross sections were normalized according to Stewart and Gabathuler. Using this procedure we find that $P_b/P \approx 1.6$ with ${}^3D$ cascade having essentially negligible effect. Thus, cascade contributes very appreciably to the polarization minimum at 26 V but is not sufficient to explain its presence.

[13] W. E. Lamb and T. H. Maiman, Phys. Rev. **105**, 573 (1957).
[14] D. Stewart and E. Gabathuler, Proc. Phys. Soc. (London) **74**, 473 (1959).

The minimum in the polarization is very curious. This line represents the only case so far discovered wherein the polarization does not monotonically fall off after reaching a maximum above threshold as the energy is decreased toward threshold. It is undoubtedly true that cascade considerably affects the shape of the polarization curve but it does not seem to offer an adequate explanation to this "anomalous anomaly." We have not resolved the $3\ {}^3P$ structure, and the $3\ {}^3P \rightarrow 2\ {}^3S$ transition has three unresolved components: $3\ {}^3P_0 \rightarrow 2\ {}^3S_1$, $3\ {}^3P_1 \rightarrow 2\ {}^3S_1$, and $3\ {}^3P_2 \rightarrow 2\ {}^3S_1$. The electron excitation cross section can be written as $Q(3\ {}^3P) = Q_0 + 2Q_1$ where Q_0 is cross section for populating states with $M_L = 0$ and Q_1 is the cross section for populating states with $M_L = \pm 1$. At threshold, $Q_1 = 0$ and the expected polarization of the $3\ {}^3P_0$, $3\ {}^3P_1$, $3\ {}^3P_2$ components will be 0, 33%, and 44.7%, respectively. One might have argued that if the energy separation between the ${}^3P_0$ and the $3\ {}^3P_{1,2}$ levels were great enough, then the electron excitation cross sections might vary enough so that the intensity ratios of components would not be constant. For instance, suppose that the ${}^3P_0$ component intensity drops off more rapidly after 26 V than expected. The polarization would then rise. This, however, seems extremely unlikely since the $3\ {}^3P_0 - 3\ {}^3P_2$ separation is more than three orders of magnitude smaller than the energy spread in the electron beam.

At higher energies, there appears a broad maximum in the polarization at about 60 V (Fig. 10). The crossover point moves to higher energies as the pressure is reduced. This may be attributed to cascade from ${}^3D$ levels.

MEASUREMENT OF GAS-KINETIC COLLISION CROSS SECTIONS

Gas-kinetic collision cross sections were determined for the $3\ {}^3P$, $4\ {}^3D$, $3\ {}^3D$, $4\ {}^1D$ and $5\ {}^1D$ levels through the use of Eq. (10) which neglects cascade effects. In
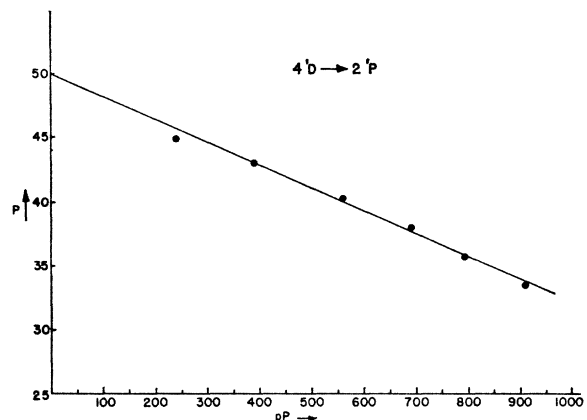

FIG. 11. Plot of the polarization (P) in $\%$ vs the product of the pressure (p) and the polarization for the $4\ {}^1D \rightarrow 2\ {}^1P$ line excited by 35-V electron impact.

TABLE I. Apparent gas-kinetic collision cross sections for various levels in helium excited by 35-V electron impact.

Level	Term value (cm^{-1})	Mean lifetime T_b $(10^{-8}$ sec)	σ_b (in units of 10^{-14} cm^2) Calculated	Experimental[a]
3 ^3P	12 746	9.66	10.3	7.2±0.9
3 ^3D	12 209	1.39	11.0	70 ±3
4 ^3D	6 866	3.23	34.0	38 ±3
4 ^1D	6 864	3.78	34.0	11.0±0.5
5 ^1D	4 392	7.27	80.0	8.3±0.7

[a] The uncertainties listed represent high confidence limits of reproducibility and are based on the assumption of zero uncertainties in the mean lifetime and in the mean thermal velocity which was taken as 1.25×10^5 cm/sec (at 20°C).

the pressure range of 0–10μ at 35 V, we found the apparent cross sections for the $3\,^3P \rightarrow 2\,^3S$, $3\,^3D \rightarrow 2\,^3P$, $4\,^3D \rightarrow 2\,^3P$, $4\,^1D \rightarrow 2\,^1P$, and $5\,^1D \rightarrow 2\,^1P$ lines to be constant. In this case, Eq. (10) can be written as $P = P_0 - \bar{v}\sigma_b T_b(nP)$. Thus, we plotted P vs nP which in each case was a good linear plot as expected (see Fig. 11). The cross section, σ_b, was determined from the slope. (The lifetime, T_b, was calculated in each case using the transition probabilities tabulated by Gabriel and Heddle.[12] The gas pressure was measured with a trapped McLeod gauge.)

To estimate the expected collision cross section it is assumed that the mean collision radius of an atom is proportional to n_{eff}^2, where n_{eff} is the effective principal quantum number which is inversely proportional to the square root of the term value of the level in question. We assume that $\sigma_b \propto (R_0 + R_b)^2$, where R_0 is the mean collision radius for an atom in the ground state and R_b is the mean collision radius for an atom in the excited level b. It follows then for collision of atoms in level b with ground state atoms that:

$\sigma_b = \frac{1}{4}\sigma_0(1 + t_0/t_b)^2$, where σ_0 is the gas kinetic collision cross section equal to about 1.5×10^{-15} cm^2. t_0 is the term value for the ground state, and t_b is the term values for level b. These are also included in Table I.

The absolute values of the cross sections calculated in this somewhat naive fashion may not be too important but it is interesting to compare them with the experimental values. One would expect an increasing trend in the experimental apparent cross section for similar spectral terms with increasing principal quantum numbers. This does not appear to be the case. The product of the lifetimes and the cross sections, which is the quantity obtained by experiment, does increase with the principal number as expected. The lifetimes shown in Table I are not expected to be too inaccurate

as shown by the lifetime measurements of Heron.[15] Thus, the decreasing trend of the experimental "cross section" with principal quantum numbers must be real. As a possible explanation we again turn to cascade. Cascade would be expected to be a larger contributor to the lower lying states which would tend to increase the apparent depolarization cross section.

THE ANOMALOUS POLARIZATION NEAR THRESHOLD

So far, experimental investigation has not resulted in a possible answer to the puzzling question of the anomalous behavior of the polarization near threshold. However, we believe that certain possibilities have been eliminated.

It appears that the presence of the anomaly is pressure independent which seemingly rules out the possibility of some pressure-dependent reaction producing the anomaly.

We believe the argument that the loss of collimation of the electron beam at lower energies is a possible cause of the anomaly is not particularly valid. In the case of $^3D \rightarrow {}^3P$ and $^1D \rightarrow {}^1P$ transitions in helium, a maximum in the polarization is reached several volts above threshold with a relatively rapid decrease in the polarization as the energy is decreased further (the classic case). In our apparatus no particular difficulty was encountered in the beam collimation until the energy was only a volt or so above threshold. Collimation could be checked instrumentally as well as visually. The beam collimation and the resolution of the two images formed by the Wollaston prism are directly correlated; thus, the recorder trace gave evidence as to the collimation when the two images were swept across the spectrometer slit.

Some concern has been expressed about the relatively large energy spread in an electron beam of this type, since the spread is much larger than the atomic energy level spacing. However, it seems to us that a reduction in the energy spread in the beam would prove advantageous only when the beam energy is very close to threshold. Since the anomaly begins to occur several volts above threshold, it seems difficult to relate the energy spread in the beam with the anomaly.

Finally, we are yet unable to offer a very satisfactory explanation of the minimum in the polarization of the $3\,^3P \rightarrow 2\,^3S$ radiation at low electron energies. We are confident that cascade greatly affects the shape of the polarization curve in this region but it does not appear to be a sufficient effect to explain this "anomalous anomaly" unless we are somehow underestimating the cascade effects from the ^3S levels.

[15] S. Heron, R. W. P. McWhirter, and E. H. Rhoderick, Proc. Roy. Soc. (London) A234, 565 (1956).